Comparative Performance Analysis of DWT- RDWT- Curvelet based Color Image Watermarking Techniques with Extraction using Independent Component Analysis

P.Mangaiyarkarasi
Assistant Professor
Dept. of E&I Engg.
Annamalai University, India.

S.Arulselvi
Professor
Dept. of E&I Engg.
Annamalai University, India.

ABSTRACT
Many literatures report about watermarking schemes based on frequency transforms like discrete wavelet transform (DWT), redundant discrete wavelet transform (RDWT) and Curvelet for gray scale images. For extraction, many of the researchers use their own extraction algorithm, which is the inverse of embedding algorithm, mainly based on embedding locations. Hence, this paper proposes robust color image watermarking techniques based on DWT, RDWT and Curvelet transform in RGB color space for copyright protection and data authentication. The proposed embedding technique is based on computation of noise visibility function (NVF), where the strength of watermarking is controlled. These results in watermarks embed at texture & edge areas are stronger than flat areas. For extraction, an intelligent detection technique, namely, fast independent component analysis (FastICA) is used. The features of FastICA are quick convergence, easy to implement and does not need original image for extracting watermark. Performances of the proposed schemes are evaluated in terms of metrics like peak signal to noise ratio (PSNR) and normalized correlation (NC) values. Robustness of the proposed scheme is validated against various image processing attacks like Gaussian noise, Salt & Pepper noise, blurring, sharpening, rotation, cropping and JPEG compression etc. The comparison analysis reveals that watermarking scheme using curvelet transform in blue plane performs superior than other transforms.

General Terms
Digital Color Image Processing, Network Security and Wavelet Applications in Digital Watermarking.

Keywords
Color Image Watermarking, Wavelet Transform, Curvelet Transform, Noise Visibility Function and Independent Component Analysis.

1. INTRODUCTION
Information is becoming widely available via global networks. Hence, the development of multimedia systems, particularly Internet is conditioned by the development of efficient methods to protect data owners against unauthorized copying and redistribution of the material on the network. Copyright protection of multimedia data has been accomplished by means of watermarking techniques. It is the process of encoding hidden copyright information within digital data by taking into account the limitations of the human audio and visual systems [1].

Watermarking techniques can be divided into two main groups: i) embedding watermarks in the spatial domain and ii) frequency domain. Spatial domain watermarking directly embeds the watermark into the object while frequency domain embeds the watermark by changing frequency component values by an orthogonal transformation. In general, the frequency domain techniques can embed more bits of watermarks and resist more attacks than spatial domain techniques. Recently the discrete wavelet transform has been used to hide data in the frequency domain. Many literatures have reported the watermarking schemes based on DWT [2, 3 & 4].

Wavelet transform has the excellent properties to minimize the data loss in the frequency transformation of images, to reduce noise and bias generation in images, and to provide extra robustness against irregular attacks. But, the DWT in watermarking is resulting with shift variant and additive noise in watermarked images. These issues can be resolved using Redundant Discrete Wavelet Transform and curvelet transform. RDWT preserves the exact edge and spectral information without much of spatial distortion. The availability of redundant data increases the robustness and imperceptibility of the watermarked image against various image processing attacks [5]. Curvelet transform brings local brightness, multiresolution, localization, directionality and anisotropy, etc. on the watermarked images and proves its superiority over the wavelet based schemes [6]. Hence, in this paper, a performance comparison is made between the three transform schemes for color images.

The need for color image watermarking is, they are everywhere in science, technology, medicine and industry. Color images are acquired and reproduced based on tristimulus values whose spectral composition is carefully chosen according to the principles of color science. Hence, the color images have to be reproduced without loss of information and to be more secure as possible. Moreover, the usage of colored data in computer networks for communication and sharing information arise the need for security. Hence, color image watermarking is an essential criterion in this digital era [7].

In [8], the algorithm selects significant DC coefficients obtained from DWT-SVD for watermark embedding. For extraction, it uses cover image and hence it is a non-blind technique. In [9], a comparative performance analysis has made between various color spaces. The decomposition is based on the combination of DWT-SVD for watermark embedding. In paper [10], input color image is split in to 3 channels R, G, B and watermark is embedded in the blue

channel. All the techniques explained uses discrete wavelet transform for the decomposition.

Hien et al proposed watermarking based on RDWT for gray level images [11]. They embed multiple watermarks on their watermarking scheme and watermarks are extracted using ICA. Mayank vatsa et al, proposes RDWT based biometric watermarking algorithm for color images. Their work focuses feature extraction and facial recognition [12]. Hein et al proposed curvelet domain based watermarking for edge embedding of gray scale images [6]. Zhiyu Zhang et al proposed a watermarking method based on curvelet for gray scale images. They embed pseudo random sequence as watermark on curvelet coefficients by sorting them based on some criteria [13].

In extraction, conventional watermark detection systems require previous knowledge of the watermark such as its location, the strength, the threshold or the original image. But the extraction based on ICA is a novel technique, which does not require the above mentioned embedding parameters. It requires watermarked coefficients and key as a mixture to extract the watermark [14].

Hence, a watermarking method for color images based on DWT, RDWT and Curvelet transforms with extraction using ICA is proposed in this paper. For watermark embedding, a perceptual model is applied with stochastic approach and it is based on computation of NVF, which has local image properties, where the strength of watermarking is controlled. The result is that watermarks at texture and edge areas are stronger than flat areas. Multiple ICA algorithms are in existence and among them, FastICA is chosen in this work, since its convergence rate is high [15, 16]. The performances of the watermarking schemes are evaluated using PSNR and NC values. Robustness and transparencies of the above schemes are demonstrated using simulation results.

The paper is organized as follows: Section 2 reviews transform techniques like DWT, RDWT and Curvelet with their tree structures and implementation. Section 3 discusses the proposed watermarking approach includes embedding and extraction procedures. Simulation results are presented in section 4 and conclusions are drawn in section 5.

2. TRANSFORM TECHNIQUES

The last two decades have seen tremendous activity in the development of new mathematical and computational tools based on multiscale ideas. Today, multiscale ideas permeate many fields of contemporary science and technology. In the information sciences and especially signal processing, the development of wavelets and related ideas led to convenient tools to navigate through large datasets, to transmit compressed data rapidly, to remove noise from signals and images, and to identify crucial transient features in such datasets.

2.1 Discrete Wavelet Transform

Wavelet transform is an information processing method and due to its capacity of multi-resolution analysis, it is particularly useful for the analysis of non-stationary signals. It has been widely used in many fields, including image processing. When an image is passed through series of low pas and high pass filters, DWT decomposes it into subbands of different resolutions [4].

A two dimensional DWT is shown in Fig. 1 .Generally, DWT decomposes an image into four non overlapping multiresolution subbands: LL1 (Approximation subband c_j), HL1 (Horizontal subband d_{hj}), LH1 (Vertical subband d_{vj}) and HH1 (Diagonal subband d_{dj}). Here, LL1 is low frequency component, whereas HL1, LH1 and HH1 are high frequency (detail) components. To obtain next coarser scale of wavelet coefficients after level 1, the sub band LL1 is further decomposed as per requirements.

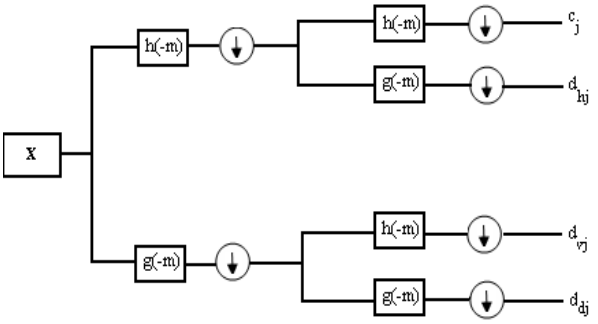

Fig 1: A two dimensional decomposition using DWT.

In Fig. 1, $h[-m]$ and $g[-m]$ are the low pass and high pass analysis filters, while the corresponding low pass and high pass synthesis filters are $h[m]$ and $g[m]$; c_j and d_j are the low band and high band output coefficients at level j.

DWT analysis is given by

$$c_{j+1}[m,n] = \left(c_j(m,n) * h[-m]\right)\downarrow 2 \quad (1)$$

$$d_{j+1}[m,n] = \left(c_j(m,n) * g[-m]\right)\downarrow 2 \quad (2)$$

Similarly DWT synthesis is given by

$$c_{j+1}[m,n] = \left[\left(c_j(m,n)\uparrow 2\right) * h[m] + \left(d_j(m,n)\uparrow 2\right) * g[m]\right] \quad (3)$$

where $*$ denotes convolution, $\downarrow 2$ and $\uparrow 2$ denotes downsampling and upsampling by a factor of two.

In a true color image, red, green and blue channels are treated individually as gray scale images and the procedure explained above is implemented separately on the color planes. Finally the three planes are concatenated to obtain watermarked image.

2.2 Redundant Discrete Wavelet Transform

Usually, watermarking performed using Discrete Wavelet Transform (DWT) preserves different frequency information in stable form and allows good localization both in time and spatial frequency domain. However, one of the major drawbacks of DWT is that the transformation does not provide shift invariance because of the down-sampling of its bands. This causes a major change in the wavelet coefficients of the image even for minor shifts in the input image. In watermarking, it is necessary the exact locations of where the watermark information is to be embedded. The shift variance of DWT causes inaccurate extraction of the watermark data and the cover image. To address the issues of DWT based watermarking, researchers have proposed the use of RDWT [12].

RDWT decomposes an image into four subbands such that the size of each subband is equal to the original image because RDWT removes the down-sampling operation from the traditional critically sampled DWT. The redundant space in this transform provides additional locations for embedding and the watermarking algorithms can be designed such that exact location of watermark embedding is preserved. To describe the implementation of the RDWT in terms of DWT is illustrated below:

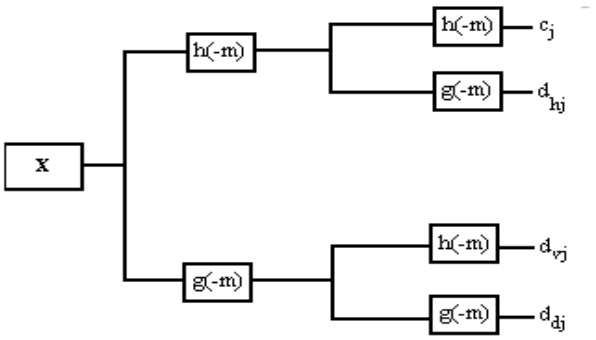

Fig 2: A two dimensional decomposition using RDWT.

In Fig. 2, the decomposition structure eliminates downsampling and upsampling of coefficients, and at each scale, the number of output coefficients doubles that of the input [17]. The filters themselves are up-sampled to fit the growing data length. Specifically, the filters for scale j are given by

$$h_j[m] = h_{j+1}[m] \uparrow 2 \tag{4}$$

$$g_j[m] = g_{j+1}[m] \uparrow 2 \tag{5}$$

The RDWT multi-resolution analysis is given by

$$c_j[m,n] = \left(c_{j+1}(m,n) * h[-m]\right) \tag{6}$$

$$d_j[m,n] = \left(c_{j+1}(m,n) * g[-m]\right) \tag{7}$$

while the RDWT synthesis is given by

$$c_{j+1}[m,n] = \frac{1}{2}\left[\left(c_j(m,n)\right) * h[m] + \left(d_j(m,n)\right) * g[m]\right] \tag{8}$$

Here also the RDWT implementation is carried over individually on three planes then concatenated to obtain watermarked color image.

2.3 Curvelet transform

Wavelet based algorithms (DWT and RDWT) have a number of advantages including time frequency localization, multiresolution representation, superior HVS modeling, linear complexity, adaptivity and it has been proved that wavelets are good at representing point wise discontinuities in one dimensional signal. However, in higher dimensions, e.g. image, there exist line or curve shaped discontinuities. Since, 2D wavelets are produced by tensor products of 1D wavelets; they can only identify horizontal, vertical, diagonal discontinuities (edges) in images, ignoring smoothness along contours and curves. Hence, curvelet transform was defined to represent two dimensional discontinuities more efficiently than the other two transforms.

Recently, Candes and Donoho [18] developed a new multiscale transform called curvelet transform, which was designed to represent edges and other singularities along with curves much more efficiently than the traditional transforms, i.e. using much fewer coefficients for a given accuracy of reconstruction. Thus, already it has been applied to processing of edge properties like noise removal [19] and contrast enhancement [20]. The following section briefly discusses the theory on curvelet transform.

2.3.1. Continuous time curvelet transform

Similar to the wavelet transform and redundant wavelet transform, the curvelet transform theory is based on sparsity theory [18]. The idea of curvelet is to calculate the inner product between an element $f \in L^2(R^2)$ and a curvelet $\varphi_{j,l,k}$.

The curvelet transform can be expressed as

$$c(j,l,k) = \left\langle f, \varphi_{j,l,k} \right\rangle = \int_{R^2} f(x)\overline{\varphi_{j,l,k}(x)}dx \tag{9}$$

here, j = 0, 1, 2, is a scale parameter; l = 0, 1, 2, is an orientation parameter; and $k = (k^1, k^2) \in z^2$ is a translation parameter. The mother curvelet is $\varphi_j(x)$, its Fourier transform is $\varphi_j(\omega) = U_j(\omega)$, where $U_j(\omega)$ is frequency window defined in the polar coordinate system such as:

$$U_j(r,\theta) = 2^{-3j/4} W(2^{-j} r) V\left(\frac{2[j/2]\theta}{2\pi}\right) \tag{10}$$

W and *V* are radial and angular windows respectively and will always obey certain admissibility conditions. Curvelet at scale 2^{-j}, orientation θ^l and position $x_k^{(j,l)} = R_{\theta_l}^{-1}(k_1.2^{-j}, k_2.2^{-j/2})$ can be expressed as:

$$\varphi_{j,l,k}(x) = \varphi_j(R_{\theta_l}(x - x_k^{(j,l)}) \tag{11}$$

So, for $f \in L^2(R^2)$, curvelet transform is expressed as:

$$c(j,l,k) := \frac{1}{(2\pi)^2} \int \hat{f}(\omega)\overline{\hat{\varphi}_{j,l,k}(\omega)}d\omega \tag{12}$$

2.3.2. Digital curvelet transform

Digital curvelet transform is linear and takes as input Cartesian arrays of the form $f[t_1, t_2]$, $0 \le t_1, t_2 < n$, which allows the output as a collection of coefficients:

$$c^D(j,l,k) := \sum_{0 \le t_1, t_2 < n} f[t_1,t_2]\overline{\varphi^D_{j,l,k}[t_1,t_2]}, \tag{13}$$

In order to improve the curvelet transform, in the sense that they are conceptually simpler, faster and far less redundant. Paper [18] proposed the Fast Discrete Curvelet Transform (FDCT) and its two digital implementations. The first is based on Un-equally-Spaced Fast Fourier transform (USFFT) while the second is based on the wrapping of specially selected Fourier samples. The FDCT-Wrapping uses simpler choice of spatial grid to translate curvelets at each scale and angle. It needs less two-dimensional FFTs than FDCT-USFFT, so it is quickly.

The architecture of FDCT via Wrapping is then roughly as follows:

1) Apply the 2D FFT and obtain Fourier sample $\hat{f}[n_1, n_2], -n/2 \le n_1, n_2 < n/2$. ($n$ is the size of the picture).

2) For each scale/angle pair (j, l), form the product $\tilde{U}_{j,l}[n_1, n_2]\hat{f}[n_1, n_2]$.

3) Wrap this product around the origin and obtain $\hat{f}_{j,l}[n_1, n_2] = W(\tilde{U}_{j,l}\hat{f})[n_1, n_2]$, where the range for n_1 and n_2 is now $0 \le n_1 < L_{1,j}$ and $0 \le n_2 < L_{2,j}$ (for θ in the range $(-\pi/4, \pi/4)$.

4) Apply the inverse 2D FFT to each, $\hat{f}_{j,l}$, hence collecting the discrete coefficients $c^D(j,l,k)$.

2.3.3. Implementation

The curvelet transform executes some processing in order to attain those properties. Fig. 3 displays the procedures for the curvelet transform. The idea is to first decompose the image into a set of wavelet bands, and to analyze each band by a local ridgelet transform. The block size can be changed at each scale level. Roughly, speaking, different levels of the multiscale ridgelet pyramid are used to represent different subbands of a filter bank output. At the same time, this subband decomposition imposes a relationship between the width and length of the important frame elements so that they are anisotropic and obey *width=length*^{2}.

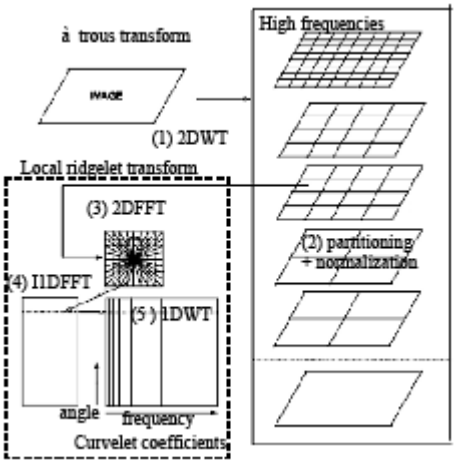

Fig 3: Representation of curvelet transform.

The implementation procedures are enumerated as follows:

1. The object is decomposed into subbands by 'a trous' transform algorithm.
2. Each subband is smoothly windowed into squares of an appropriate scale.
3. Each square is analyzed via the discrete ridgelet transform [21].

In this definition, the two dyadic subbands [$2^{2s;}$ 2^{2s+1}] and [2^{2s+1} ; 2^{2s+2}] are merged before applying the ridgelet transform. In the result, the curvelet coefficients are obtained with involvement of edge information as shown in Fig. 3. The above procedure is implemented on three color planed of a color image , then merged together to obtain watermarked image.

3. PROPOSED SCHEME

The proposed scheme separates red, green and blue planes from the host image and embeds the watermark on blue channel. The scheme uses a binary image as watermark. The procedure for embedding and extraction is described briefly in the following section.

3.1 Watermark embedding

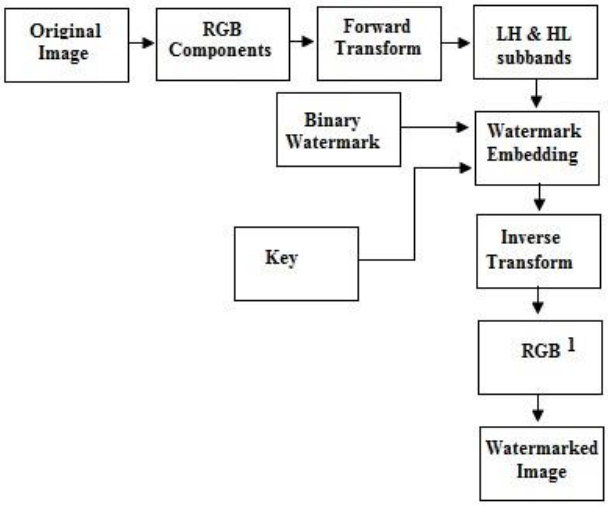

Fig 4: Watermark embedding procedure.

The proposed watermark embedding algorithm is shown in Fig.4. The steps of watermark embedding algorithms are as follows:

Step 1: Separate R, G and B components from the host image.

Step 2: Select blue component and apply forward transforms (DWT, RDWT and Curvelet) to obtain frequency domain coefficients for watermark embedding.

Step 3: Compute NVF for the original image using the formula

$$NVF(i,j) = \frac{1}{1+\sigma_x^2(i,j)} \qquad (14)$$

where $\sigma_x^2(i,j)$ denotes variance of the cover image in a window centered on the pixel with coordinates (i,j). By applying NVF, the watermark in texture and edges becomes stronger than in flat areas. Fig. 5 shows the NVF of Lena image.

Fig 5: NVF of Lena image.

Step 4: The watermark embedding formula is given by

$$I'LH_2(i,j) = LH_2(i,j) + E(LH_2)\alpha_1(1 - NVF(i,j))W(i,j) + \frac{E(LH_2)}{10}.\alpha_2.NVF(i,j).W(i,j) \quad (15)$$

where $I'LH_2(i,j)$ and $I'HL_2(i,j)$ are watermarked transform coefficients, $E(LH_2)\alpha_1$ and $E(HL_2)\alpha_1$ denote the watermark strengths of texture and $\frac{E(LH_2)}{10}.\alpha_2$ and $\frac{E(HL_2)}{10}.\alpha_2$ denote the watermark strengths of edge regions for LH and HL subbands, respectively. α_1 and α_2 are smoothing factors at the texture regions and flat regions, E denotes the mean and $W(i,j)$ is the watermark.

Step 5: Perform inverse of the transforms mentioned in step 2 with the help of watermarked coefficients.

Step 6: Concatenate watermarked blue component along with red and green components to obtain watermarked color image.

3.2 Watermark extraction

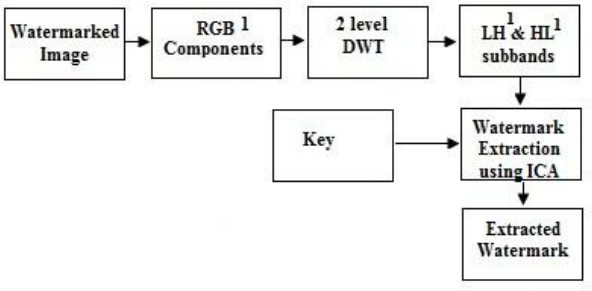

Fig 6: Watermark extraction procedure.

The watermark extraction algorithm is shown in Fig. 6. The steps of watermark extraction algorithm are as follows:

Step 1: During extraction, the watermarked image is again separated into R, G, B components and B component is forward transformed as mentioned earlier.

Step 2: From the resultant subbands, the watermarked coefficients along with key are used to generate input mixture for ICA is given by

$$X_1 = a_{11}I' + a_{12}W + a_{13}K \quad (16)$$

$$X_2 = a_{21}I' + a_{22}W + a_{23}K \quad (17)$$

$$X_3 = a_{31}I' + a_{32}W + a_{33}K \quad (18)$$

where X_1, X_2, X_3 are mixtures, I' is the watermarked image, $\boldsymbol{a}$ is a mixing matrix, W is the encrypted watermark matrix and K is a random key in the embedding process.

Step 3: Apply ICA on these mixtures to extract the watermark from the watermarked image. Since ICA doesn't require original image for extraction, the proposed extraction is said to be blind.

3.2.1 Independent Component Analysis (ICA)

This section briefly reviews ICA algorithm and how ICA is applied to watermark extraction. It is a novel statistical technique that aims at finding linear projections of the data that maximize their mutual independence. ICA has received attention because of its potential applications in signal processing such as in feature extraction, and blind source separation with special emphasis to physiological data analysis and audio signal processing. The goal of ICA is to recover the source signals from the sensor observations that are linear mixtures of independent source signals. It aims at extracting unknown hidden components from multivariate data using only the assumption that the unknown factors are mutually independent [14].

ICA has several forms of implementations and one among them is FastICA whose algorithm is outlined as follows:

i) The mean of the mixed signal X is subtracted so as to make X as a zero mean signal as $X = X - E[X]$, where $E[X]$ is the mean of the signal.

ii) Then covariance matrix $R = E[XX^T]$ is obtained and eigenvalue decomposition is performed on it is given by, $R = EDE^T$, where E is the orthonormal matrix of eigenvalues of R and D is the diagonal matrix of eigenvalues.

iii) Find the whitening matrix, P which transforms the covariance matrix into an identity matrix and it is given by $P = Inv\left(sqrt(D) \times E^T\right)$.

iv) Choose an initial weight vector W, such that the projection $W^T X$ maximizes non gaussianity as

$$W^+ = E\{X * g(W^T X)\} - E\{g'(W^T)\}W \quad (19)$$

where 'g' is the derivative of the nonquadratric function.

v) The variance of $W^{+T} X$ must be made unity. Since X is already whitened it is sufficient to constrain the norm of W^+ to be unity.

$$W = W^+ / \|W^+\| \quad (20)$$

If W not converges means go back to step (iv).

vi) The demixing matrix is given by

$$W = W^T \times P \quad (21)$$

and independent components are obtained by

$$\bar{S} = W \times X \quad (22)$$

In this work, a linear mixture of watermarked image with key is generated as input signal to the ICA and the ICA separates the watermark as the output from the mixtures. The novelty of

this detector is, that it does not require original image and embedding parameters such as watermark location and strength. Moreover, it is fast in convergence, easy to implement and suitable for watermarking applications.

4. SIMULATION RESULTS

The simulation results of the watermarking techniques are analyzed with standard test images Lena, Peppers, Barbara and Moon. A binary image 'aulogo' is used as the watermark. The original images are shown in Fig. 7.

First, the simulation is carried out with DWT technique. From the true color image, Red, green and Blue components are separated as shown in Fig. 8. The embedding algorithm based on DWT is implemented on three channels individually and the quality of watermarked images is evaluated through PSNR values. The values obtained are given in Table 1 and the results reveal that blue channel produces the maximum PSNR values when compared to red and green channels for all test images.

The same set of experimentation is carried out using RDWT and curvelet transform, their corresponding PSNR values are presented in Table 2 and Table 3 respectively. The results strengthen the conclusion that blue channel retain the energy of the signal by producing high PSNR values in these transforms also. The reason behind this is the correlation for blue channel is less than the other color components. The quality of extracted watermark is evaluated by comparing it with the original watermark in terms of Normalized Correlation (NC) values.

Table 4, 5 and 6 shows the normalized correlation (NC) values calculated between original and extracted watermarks with DWT, RDWT and Curvelet schemes. NC values represent the degree of similarity between the two watermarks and it ranges from 0 to 1, as 0 implies no similarity where 1 represents exactly the two watermarks are equal. Even though there is not much difference between the R, G & B channels, the watermark extracted from the blue channel is almost similar to original watermark than other channels. In curvelet transform particularly, NC values attain its maximum value 1 for Lena, Peppers and Barbara images, where Moon has 0.99.

Fig. 9 shows the simulation results of the three schemes for three color channels. Fig. 9 (a) shows the watermarked images obtained by DWT scheme for the three color channels Red, Green and Blue. Among the three, the clarity of watermarked image in blue channel is comparatively better than other channels. The sharp edges and fine details get blurred in Red and Green channels are visually clear. Fig. 9 (b) shows the corresponding extracted watermarks of these three color channels by DWT scheme. Even though they are seem to be identical, minor features get enhanced in blue channel than others. Similarly, in the other two schemes also, blue channel performs better in embedding as well as extraction is proven from the results.

With these results, this paper work recommends watermarking on blue channel perform better for copyright protection and authentication purpose. For further experimentation i.e. to compare the transformations, watermark is embedded and extracted on blue channel.

Table 1. PSNR (dB) values for various images by DWT

Images	Red	Green	Blue
Lena	39.5896	39.4929	**40.1007**
Peppers	39.3082	39.6495	**40.0059**
Barbara	38.3251	38.4082	**38.4638**
Moon	39.9598	39.9129	**40.0589**

Table 2. PSNR (dB) values for various images by RDWT

Images	Red	Green	Blue
Lena	50.8393	50.5919	**51.2171**
Peppers	51.8213	52.2246	**52.4348**
Barbara	49.5576	49.6923	**49.8542**
Moon	51.6967	51.3600	**51.3919**

Table 3. PSNR (dB) values for various images by Curvelet

Images	Red	Green	Blue
Lena	62.6591	59.7260	**64.5796**
Peppers	61.8350	62.0797	**62.5347**
Barbara	59.3718	60.7801	**62.7367**
Moon	63.0096	62.8150	**63.2485**

Table 4. NC values for various images by DWT scheme

Images	Red	Green	Blue
Lena	0.9067	0.9069	**0.9076**
Peppers	0.9077	0.9079	**0.9083**
Barbara	0.9073	0.9077	**0.9080**
Moon	0.9081	0.9079	**0.9078**

Table 5. NC values for various images by RDWT scheme

Images	Red	Green	Blue
Lena	0.9514	0.9516	**0.9518**
Peppers	0.9514	0.9518	**0.9519**
Barbara	0.9514	0.9517	**0.9517**
Moon	0.9518	0.9518	**0.9518**

Table 6. NC values for various images by Curvelet scheme

Images	Red	Green	Blue
Lena	1.0000	.9982	**1.0000**
Peppers	1.0000	1.0000	**1.0000**
Barbara	1.0000	1.0000	**1.0000**
Moon	0.9523	0.9399	**0.9889**

(a) Lena

(b) Peppers

(c) Barbara

(d) Moon

(e) Binary watermark (aulogo)

Fig 7: Input images.

(a) Red

(b) Green

(c) Blue

Fig 8: Color components of Lena image.

Red Green Blue

(a) Watermarked images by DWT

Red Green Blue

(b) Extracted watermarks by DWT

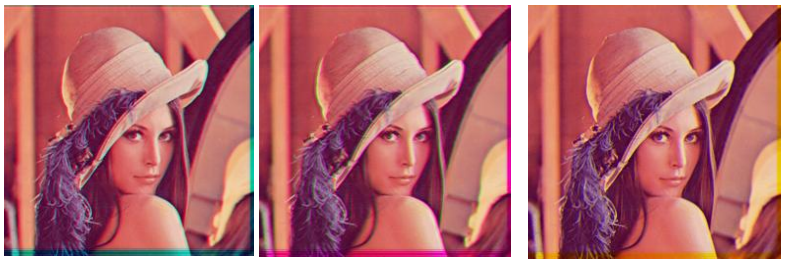

Red Green Blue

(c) Watermarked images by RDWT

Red Green Blue

(d) Extracted watermarks by RDWT

Red Green Blue

(e) Watermarked images by Curvelet

Red Green Blue

(f) Extracted watermarks by Curvelet

Fig 9: Watermarked images and corresponding extracted watermarks by DWT, RDWT, Curvelet schemes.

Table 7 compares the performance of the transforms DWT, RDWT and curvelet through PSNR values. Fig. 12 shows the watermarked images of Lena, Peppers, Barbara and Moon obtained by these schemes. Although DWT preserves information in both spatial and frequency aspect, the downsampling operation during decomposition leads to information reduction. Due to that, DWT fails to represent the edges and fine details in watermarked image. These issues can be overcome by RDWT.

The PSNR values mentioned in Table 7 clearly shows the difference between two techniques. For Lena image, PSNR values increased to 51.2171(RDWT) from 40.1007 (DWT). This due to the redundant data generated during RDWT decomposition where there is no downsampling operation. This redundant data increases the number of coefficients required for reconstruction of the image. Hence, the quality of watermarked image increases considerably both visually as well as statistically.

Some images have to be represented by line singularity instead of point singularity. Such circumstances, wavelet based schemes both DWT and RDWT are failed to perform in an effective way. Curvelet transform may be a good choice to represent line singularity; hence, it enables most of the energy of the object to be localized in just a few coefficients. The optimally sparse representation of image edges allows the transform to embed watermarks and recover watermarks from severe image degradation.

Table 7 also compares the performance of watermarked scheme by curvelet with RDWT and DWT. From the results, curvelet transform performs the best in providing maximum PSNR values. The quality of watermarked image is improved to a high extent. Fig. 10 shows the performance comparison of the three schemes in a plotted manner.

Table 8 compares the extraction performance of the 3 schemes using NC values. Once again it is proved that the extraction of watermarks by curvelet is almost equal to the original watermark where DWT and RDWT possess 95% and 90% similarity. Fig. 11 shows the performance comparison of the three schemes in a plotted manner. It is concluded that curvelet is the optimum choice for watermarking purpose.

Table 7. PSNR (dB) values for various images by DWT, RDWT and Curvelet schemes

Images	DWT	RDWT	Curvelet
Lena	40.1007	51.2171	**64.5796**
Peppers	40.0059	52.1348	**62.5347**
Barbara	38.4638	49.8542	**59.7367**
Moon	39.9598	51.3919	**63.2485**

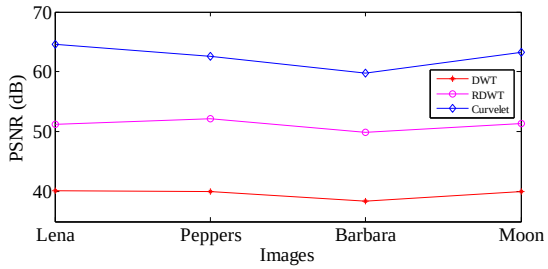

Fig 10: Comparison of PSNR (dB) values of the three schemes for various input images.

Table 8. NC values for various images by DWT, RDWT and Curvelet schemes

Images	DWT	RDWT	Curvelet
Lena	0.9076	0.9518	**1.0000**
Peppers	0.9083	0.9519	**1.0000**
Barbara	0.9080	0.9517	**1.0000**
Moon	0.9080	0.9518	**0.9889**

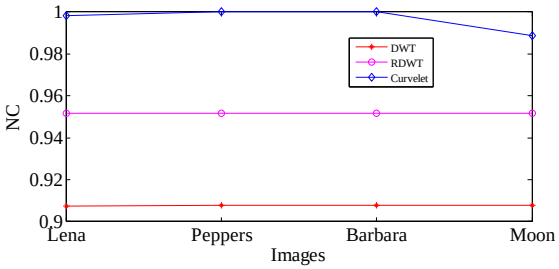

Fig 11: Comparison of NC values of the three schemes for various input images.

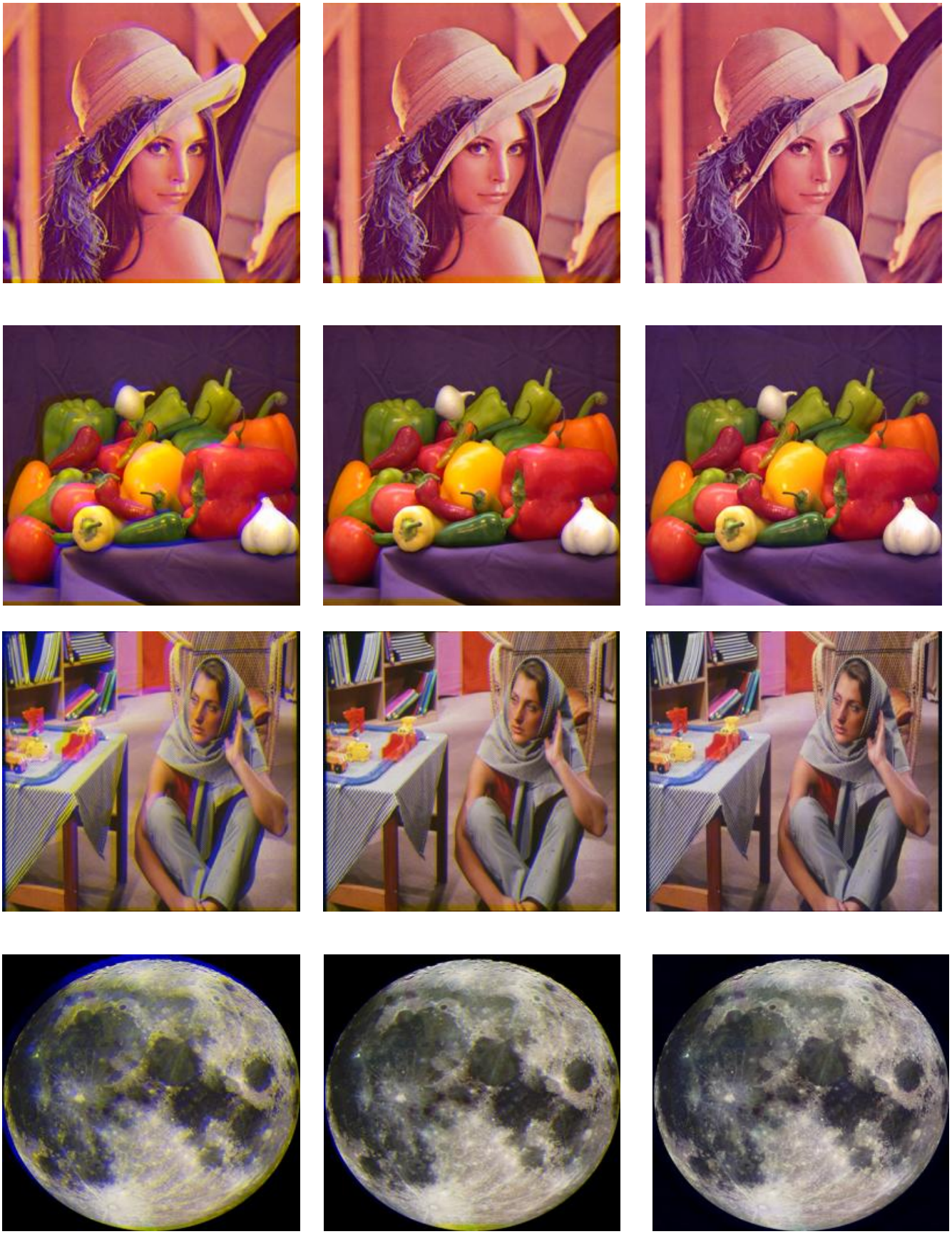

Fig 12: Watermarked images obtained by DWT, RDWT and Curvelet schemes for different input images.

The robustness of the proposed scheme is validated against attacks like Gaussian noise addition, Salt & Pepper noise addition, Blurring, Sharpening, Rotation, Cropping and JPEG Compression. Fig. 13 shows the watermarked images obtained by the three transform techniques after implementing the above mentioned attacks. Their extracted watermarks from the respective images are also shown in the same. Fig. 13(a) shows the watermarked image added with Gaussian noise of zero mean and variance 0.1. Fig. 13(b) shows the watermarked image added with Salt & Pepper noise with noise density 0.1. Fig.13 (c) and (d) show the blurred and sharpened images respectively by a factor of 0.2. Blurring operation uses averaging filter where sharpening uses high pas filter. Fig. 13 (e) shows the rotated image by 10 deg. Fig. 13(f) shows the watermarked image with 25% corner cropping, where the pixels of the watermarked image are replaced by zeros. Fig. 13(g) shows the JPEG compressed image with compression ratio 20. The PSNR and NC values calculated after the above mentioned attacks are tabulated in Table 9 and 10. Fig. 14 and 15 represents the statistical values of the table as bar graphs.

From the results, two points to be notified: First one is Curvelet transform performs the best in surviving against attacks by producing high PSNR values when compared to other transforms. Hence, it retains the pixels that required for reconstruction thus producing a qualified image. Second, the watermarks embedded can almost extract perfectly in Curvelet domain. In the presence of attacks, the degree of similarity between original and extracted watermark is 83% in DWT scheme, 90% in RDWT scheme and 99% in Curvelet scheme. The availability of enormous data makes the extractor (ICA) to perform better in Curvelet transform. Hence, its performance is superior.

Table 9. Robustness of the transforms against attacks in terms of PSNR values (Lena)

Attacks	DWT	RDWT	Curvelet
Gaussian noise	18.2539	28.2604	**30.5443**
Salt & Pepper noise	19.6971	30.5639	**36.3751**
Blurring	19.0442	29.7238	**34.6084**
Sharpening	19.0307	29.6664	**34.5857**
Rotation	16.9606	26.7378	**27.5187**
Cropping	17.6709	28.1521	**29.9152**
JPEG compression	17.4536	20.2047	**25.7891**

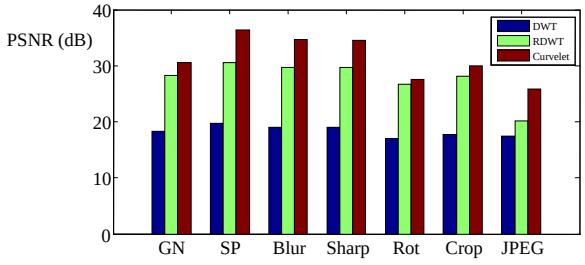

Fig 14: Comparison of PSNR values of the three schemes for various attacks.

Table 10. Extraction performance of the transforms in the presence of attacks in terms of NC values (Lena)

Attacks	DWT	RDWT	Curvelet
Gaussian noise	0.8308	0.9079	**0.9920**
Salt & Pepper noise	0.8283	0.9062	**0.9925**
Blurring	0.8302	0.9071	**0.9925**
Sharpening	0.8301	0.9073	**0.9921**
Rotation	0.8322	0.9087	**0.9978**
Cropping	0.8320	0.9086	**0.9960**
JPEG compression	0.8324	0.9088	**0.9888**

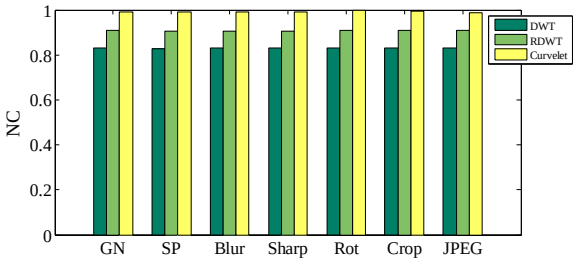

Fig 15: Comparison of NC values of the three schemes for various attacks.

5. CONCLUSION

(i) A comparative performance analysis of DWT-RDWT-Curvelet based watermarking algorithms for color images is presented in this paper.

(ii) Watermark is embedded in Red, Green and Blue channels individually using three transform methods.

(iii) For extraction, an intelligent, fast and blind detector ICA is used.

(iv) Watermarks are extracted from Red, Green and Blue channels of the watermarked images obtained using three transforms.

(v) From the results, it is observed blue channel produces maximum PSNR values as well as NC values for various input images.

(iv) Robustness of the overall technique is validated against attacks like Gaussian noise, Salt& Pepper noise, Blurring, Sharpening, Rotation, Cropping and JPEG Compression.

(v) In the presence of attacks, the performance of curvelet based scheme is superior when compared to other transforms in both embedding as well as extraction.

Hence, it is concluded that curvelet based watermarking scheme on blue component of a color image performs better in watermarking purpose. Curvelet transform based color image watermarking may be a viable solution for copyright protection and content authentication.

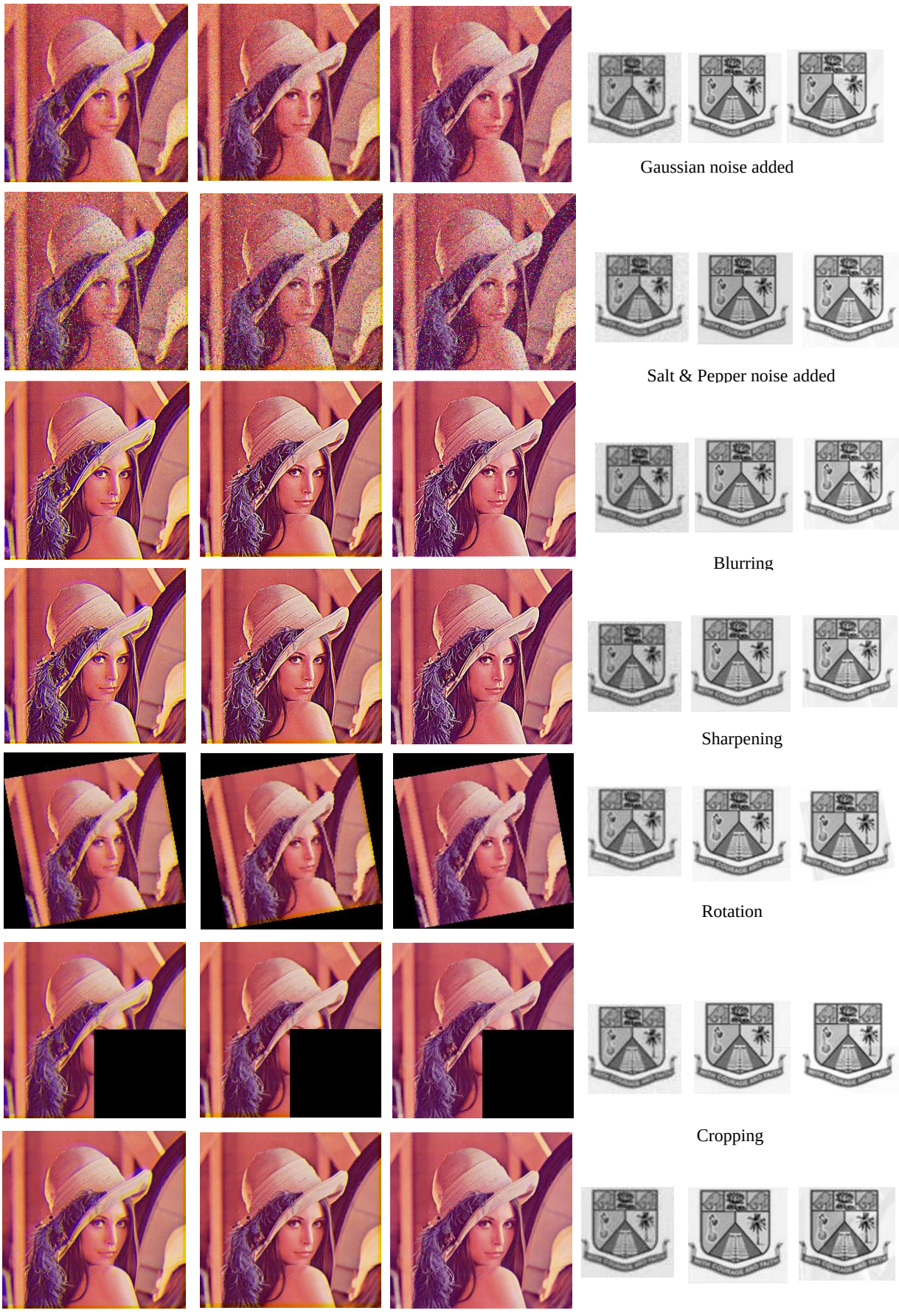

Fig 13: Various attacks on watermarked images (DWT, RDWT& Curvelet) and their corresponding extracted watermarks.

6. REFERENCES

[1] Wie-Bin Lee and Tung-Her Chen. 2002. A public verifiable copy protection technique for still images. Elsevier Journal of Systems and Software, vol.62, pp. 195-204.

[2] Barni M., Bartolini A. and Piva. 2001. Improved wavelet based watermarking through pixel wise masking. IEEE Transactions on Image Processing, vol.10, no.5, pp.783-791.

[3] Paquet A. and Ward R. 2002. Wavelet based digital watermarking for image authentication. In Proceedings of IEEE Canad. Conference on Electrical and Computer Engineering, vol. 2, pp. 879-884.

[4] Mangaiyarkarasi P. and Arulselvi S. 2012. A robust digital image watermarking technique based on DWT and FastICA. CIIT International Journal of Digital Image Processing, vol. 4, no. 2, pp. 100-105.

[5] Thirugnanam G. and Arulselvi S. 2010. RDWT based digital image watermarking and extraction using independent component analysis. International Journal of Image Processing, vol.2, no.3, pp. 111-118.

[6] Hien T.D.,Hanane Hark, Yen Wei Chan and Yasunori Nagata. Curvelet domain image watermarking based on edge embedding.-------

[7] Rafael C. G. and Richard E.W. 2002. Digital Image Processing. Second Edition. Pearson Education.

[8] Shanthi V. and Arunkumar T. 2011. DC coefficients based watermarking technique for color images using singular value decomposition. International Journal of Computer and Electrical Engineering, vol. 3, no. 1, pp. 8-16.

[9] Baisa L. G and Suresh N. M. 2011. Comparative performance analysis of DWT-SVD based color image watermarking technique in YUV, RGB and YIQ color spaces. International Journal of Computer Theory and Engineering, vol.3, no. 6, pp. 714-717.

[10] Mangaiyarkarasi P. and Arulselvi S. 2012. Robust color image watermarking technique based on DWT and ICA. International Journal of Computer Applications, vol. 44, no. 23, pp. 6-12.

[11] Hien T. D., Zensho Nakao and Yen-Wei Chen. 2006. Robust multilogo watermarking by RDWT and ICA. Elsevier Journal on Signal Processing, vol.86, pp. 2981-2993.

[12] Mayank Vasta, Richa Singh and Afzel Noore. 2009. Feature based RDWT watermarking for multimodal biometric system. Elsevier Journal on Image and Vision Computing, vol.27, pp. 293-304.

[13] Zhiyu Zhang, Wei Huang, Jiulong Zhang, Haiyan Yu, and Yanjun Lu. 2006. Digital image watermark algorithm in the curvelet domain. Intelligent Information Hiding and Multimedia Signal Processing. pp. 105-108.

[14] Hyvarinen A., Karhunen J., and Oja E.1999. Independent Component Analysis. First Edition, John Wiley & Sons.

[15] Thirugnanam G. 2011. Certain investigations on wavelet based watermarking algorithms for images. Doctoral Thesis, Dept. of E&I Engg., Annamalai University.

[16] Thirugnanam G., Natarajan M., Mangaiyarkarasi P., and Malmurugan N. 2009. Comparison of independent component analysis for DWT based digital image watermarking. International Journal of Advance Research in Computer Engineering, vol. 3, no. 1, pp.165-169.

[17] Mangaiyarkarasi P. and Arulselvi S. 2012. Improved performance by parametrizing wavelet filters for digital image watermarking. Signal & Image Processing: An International Journal, vol. 3, no. 1, pp. 29-38.

[18] Candes E.J., Demanet L., Donoho D. and Ying L. 2006. Fast Discrete Curvelet Transforms. Technical Report, California Institute of Technology.

[19] Starck J.L., Candes E.J, Donoho D. and Ying L. 2002. The curvelet transform for image denoising. IEEE Transactions on Image Processing, vol.11, no.6, pp.670-684.

[20] Starck J.L., Murtagh F., Candes E.J, and Donoho D. 2003. Gray and color image contrast enhancement by the curvelet transform. IEEE Transactions on Image Processing, vol.12, no.6, pp.706-717.

[21] Minh N.D. and Martin Vetterli. 1997. The finite ridgelet transform for image representation. IEEE Transactions on Image Processing.

AUTHORS PROFILE

P.MANGAIYARKARASI received her B.E., Electronics & Instrumentation, from Annamalai University in 1999 and M.E., Process control and Instrumentation from Annamalai University in 2001. Currently she is doing Ph.D. in the area of Digital Image Watermarking. At present she is working as Assistant Professor in the Dept. of E&I Engg., Annamalai University. Her research interests include Digital Signal Processing, Digital Image Processing and Digital Watermarking.

S.ARULSELVI received her B.E., Instrumentation & Control from GCT, Coimbatore in 1988, M.E., Control and Instrumentation from Anna University in 1998 and Ph.D. in Power Electronics from Anna University in 2007. Currently she is working as Professor in the Dept. of E&I Engg., Annamalai University. Her area of interests includes Digital Watermarking, Image Processing, Power Electronics and Control etc.